ARTICLE

C−S Activation of CS_2 by Nb^+ in Gas Phase

Xiao-li Song, Li-guo Gao*

College of Chemistry and Chemical Engineering, Yulin College, Yulin 719000, China

(Dated: Received on November 22, 2008; Accepted on January 6, 2009)

The reaction of Nb^+ with CS_2, producing cationic transition-metal sulfide and CS, was taken as a representative example to elucidate the overall mechanism of reactions of second-row early transition metal ions with CS_2. The reactions in both triplet and quintet state were studied by using the UB3LYP density functional method with the Stuttgart pseudo potentials and corresponding basis sets for Nb^+ and the standard 6-311+G(2d) basis sets for C and S. The geometries for reactants, the transition states, and the products were completely optimized. All the transition states were verified by vibrational analysis and intrinsic reaction coordinate calculations. The results show that the reaction mechanism between niobium ion and CS_2 is an insertion-elimination mechanism. Intersystem crossing may occur in the reaction Nb^+ with CS_2 and a minimum energy crossing point was found.

Key words: Second-row early transition metal ion, Reaction mechanism, Intersystem crossing, Minimum energy crossing point

I. INTRODUCTION

Transition metal sulfides play a significant role in industrial, biological, and geological systems [1-4]. In many biological systems, it has been found that sulfur coordination is necessary for the functioning of numerous biological transition metal centers [5]. The sulfides are less reactive than their corresponding oxides. However, sulfides get more attention because of their higher selectivity and greater resistance against catalysis poisoning than the corresponding oxide catalysts [6]. CS_2 is an important sulfur-transfer reagent [7]. The reactions of some transition metal ions of the first series with CS_2 have been studied both by theory and experiment [8-13], and it was found that the reactions of M^+ (M^+=Sc^+, Ti^+, V^+, Fe^+, Cu^+, and Zn^+) with CS_2 are spin-forbidden for formation of ground state products from ground state reactants both in the experiments and theory. Can a reaction mechanism similar to that for the reactions of first row transition metal ions with CS_2 be applicable to second row transition ions? Although some second-row transition metal ion-CS_2 reactions have been investigated experimentally [14], and accurate thermochemical data has been obtained, detailed information of the potential energy surface of $[Nb, C, S]^+$ is still scarce. Further, confirmation of the relevant mechanism needs the assistance of theory. The application of quantum mechanical calculations to these compounds is more difficult than to other branches of chemistry because many reactions of transition metal ions involve low-lying excited electronic states [11-13,15-19]. In these cases, the corresponding stationary points governing chemical reactivity lie on different potential energy surfaces (PESs), and this fact opens the possibility of a nonadiabatic behavior, in which the more favorable pathway does not remain on a single PES. Some chemists call such a phenomenon "two-state reactivity" (TSR) [15]. In these reactions, the reaction rate can be limited by the transition structure (TS) on the PES for either electronic state and by the rate of crossing between surfaces. Therefore, it is necessary to locate and characterize the stationary points on each PES and the key regions of the PESs where the relevant spin states lie close in energy and geometry, corresponding to the crossing point (CP). In order to better understand the mechanism of the Nb^+ and CS_2 reaction, we obtain a minimum energy crossing point (MECP), and discuss potential surface crossing and possible spin-inversion processes in this intriguing chemical reaction in this work.

II. CALCULATION METHODS

Computations were carried out with the Gaussian 03 package of programs [20]. The fully optimized geometries and the vibrational frequencies have been determined using the three-parameter hybrid B3LYP density method [21,22]. This choice was motivated by its successful performance for many open-shell transition metal compounds [23,24]. The basis set used consists of the relativistic effective core potential (ECP) of Stuttgart on transition metal ions.

The 4d and 5s in transition metal ions are treated

*Author to whom correspondence should be addressed. E-mail: liguogao2008@163.com, liguogao2008@yahoo.com.cn, Tel.: +86-912-3891144.

TABLE I Theoretical and experimental bond dissociation energies at 0 K (in kJ/mol).

Species	Calculation				Experiment
	BP86	BLYP	B3P86	B3LYP	
OC−S	345.5	316.1	327.4	299.2	302.2±0.5 [31]
SC−O	715.5	687.8	697.5	666.9	661.9±3.8 [31]
SC−S	476.1	446.4	465.3	440.6	433.0±3.8 [31]
C−S	725.9	699.6	697.5	677.4	709.2±3.8 [32]
Nb^+−S	507.9	610.0	443.1	448.1	502.2±20.3 [14]
Nb^+−CS	441.0	342.3	262.7	250.8	242.4±10.6 [14]

explicitly by a (8s7p6d) Gaussian basis set contracted to [6s5p3d]. For C and S, we used the 6-311+G(2d) basis set. All stationary points were characterized by vibrational analysis and the zero-point energy (ZPE) corrections were included. The transition state structures all represent saddle points, characterized by one negative eigenvalue of the Hessian matrix. To ensure reliability of the reaction path, the pathways between the transition structures and their corresponding minima were characterized by internal reaction coordinate (IRC) calculations [25].

Energy surface crossings play important roles in understanding chemical reactivity when a process involves a change in the total electronic spin. Determining the lowest CP at which two energy surfaces corresponding to different spin states intersect with minimum energy is fundamental because it is the most likely place for the transition to occur [26]. To localize and characterize the CP, the concept of MECP on the seam line at which two electronic surfaces of different spin multiplicities intersect is used. Therefore, all coordinates were optimized in searches for the CP between the two PESs in which DFT energies and gradients were calculated for each spin multiplicity. Starting from the TS closest to the crossing seams, the reaction pathway was traced down to the corresponding minimum. Thereafter, each optimized point along the IRC path was submitted to a single-point energy calculation with the other electronic state. The CP that we obtain in this way can be considered as an estimate of the MECP between the two hypersurfaces. For the sake of comparison, the mathematical algorithm to MECP developed by Harvey *et al.* was employed [27-29], and the MECP was optimized with a separate program linked to the Jaguar QM software. The MECP program extracts gradients from the Jaguar calculations and uses them to construct an effective gradient pointing toward the MECP. The energy convergence criteria is 10^{-4} Hartree (0.25 kJ/mol) [30].

III. RESULTS AND DISCUSSION

In the following sections, we will first establish the accuracy that can be expected from the chosen B3LYP functional for the Nb^++CS_2 system. Then, we will present the theoretical results for various intermediates, TS, and products involved in the reaction of Nb^+ with CS_2, and discuss the mechanisms of C−S bond activations in light of the recent experimental and theoretical data available.

A. Evaluation of the computational accuracy

In recent years, DFT [9-12,33-36] has attracted considerable attention and has been widely applied to electronic structure calculations for systems containing transition metals. DFT methods have been shown to be particularly useful and computationally efficient for systems with a relatively large number of electrons. To find a reliable functional for describing the present Nb^++CS_2 system, we calculated the bond dissociation energies (BDEs) of OCS and several species involved in the reaction of Nb^+ with CS_2 using several popular functionals: B3LYP, BLYP, B3P86, and BP86. The relevant results are shown in Table I, where available experimental values are also listed for comparison.

By comparing these theoretical values with experimental findings, we found that B3LYP and B3P86 functionals gave relatively smaller absolute errors than BLYP and BP86 functionals. Therefore, the calculated results from B3LYP and B3P86 can be considered satisfactory, considering our main goals in the present work are the examination of the detailed reaction mechanism and the calculation of the relative energies of the species involved, not the calculation of accurate bond energies. On the other hand, B3LYP DFT method is motivated by its extensive use in the latest literature as a practical tool in describing open-shell transition metal compounds [9-12,16].

Previous investigations of transition metal compounds also underlined the reliability of B3LYP for describing PESs as well as predicting electronic structures and thermochemical properties. On the basis of the facts mentioned above, we are confident in the ability of the B3LYP functional to describing the features of the PES of $[Nb, C, S]^+$.

B. Overall features of reactions

Figure 1 shows the optimized geometries of the reagents, the encounter complexes, the products, and

DOI:10.1088/1674-0068/22/03/297-302

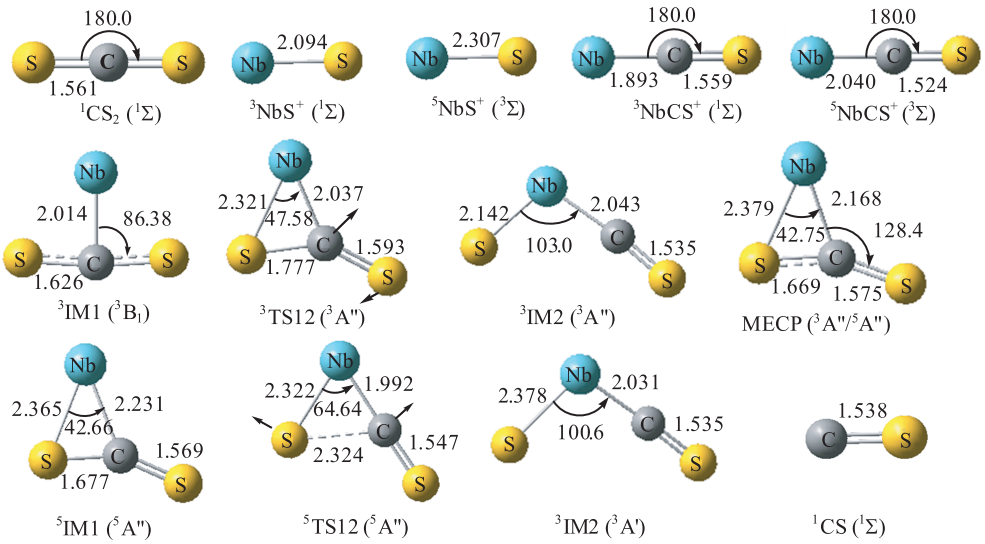

FIG. 1 Optimized geometrical parameters for the reactants, products, intermediates, saddle points and MECP. Distances in Å and angles in (°).

the transition states along the preferred reaction pathway in the high spin quintet and low-spin triplet states. Important atomic distances and bond angles are indicated in these illustrations. Transition vectors and corresponding imaginary frequencies are shown in the TS structures. We inspected the values of $\langle S^2 \rangle$ for all species involved in the reactions of Nb^+ with CS_2, and found the deviation of $\langle S^2 \rangle$ is less than 5%. The fact indicates that spin contamination is small in all of the calculations.

We originally assumed that there are two reasonable mechanisms for the interaction of Nb^+ and CS_2: the Nb^+ insertion into a C−S bond to form a S−Nb^+−C−S intermediate, or direct abstraction of the S atom from CS_2. The latter turns out to be unsuccessful, that is, the reaction mechanism Nb^++CS_2 is an insertion-elimination mechanism.

Structures ^{3}IM1 and ^{5}IM1 (where the superscripts 3 and 5 denote the spin multiplicity) are the initial complexes formed as Nb^+ and CS_2 approach each other. They have different structure and symmetry. ^{3}IM1 has C_{2v} symmetry and ^{5}IM1 has C_s symmetry. It is clear that in ^{3}IM1 the Nb^+ coordinates to atom C, whereas in ^{5}IM1 it coordinates to atom C and S in CS_2. The Nb−C distances in ^{3}IM1 and ^{5}IM1 are 2.014 and 2.231 nm, respectively. ^{3}IM1 and ^{5}IM1 are more stable than the ground state of the reactants Nb^++CS_2 by 225.9 and 159.0 kJ/mol, respectively. Obviously, the ground state of IM1 is in its triplet (Fig.2).

Along the reaction coordinate, intermediate IM1 can be converted into an insertion species of Nb^+ into the C−S bond, intermediate IM2. As shown in Fig.1, the geometries of IM2 on the quintet and triplet surfaces are similar. We found that the ground state of the inserted intermediate is a triplet. The transformation of the encounter complex Nb^+−SCS (IM1) into the inserted structure SC−Nb^+−S (IM2) proceeds through the transition state called TS12, which has been confirmed by the IRC calculations. Structurally, they are three-membered-ring transition states with C_s symmetry. The energy of the ^{3}TS12 is located at 71.9 kJ/mol above the ^{3}IM1, and the corresponding imaginary frequency is 334i cm^{-1}. The intermediate ^{5}IM1 and the inserted complex S−Nb^+−CS(^{5}IM2) are connected by ^{5}TS12. The corresponding imaginary frequency is 272i cm^{-1}, and the normal modes correspond to the C−S bond rupture. Once IM2 is formed, two exit channels are open (see Fig.1 and Fig.2). All the products observed in the experiment can be explained by the cleavages of different bonds in this insertion species. The energetically most favorable channel is to form the dissociation products of NbS^+ and CS through the cleavage of Nb−C bond in IM2, which is exothermic by 2.9 kJ/mol

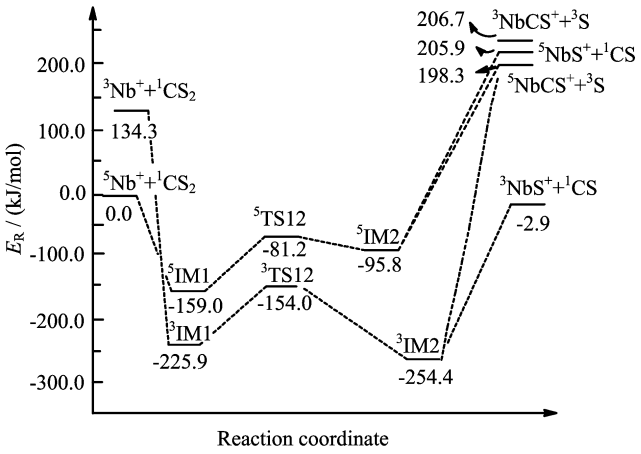

FIG. 2 Diagram of the reaction path channels for the reaction Nb^++CS_2 at UB3LYP level of calculations.

DOI:10.1088/1674-0068/22/03/297-302

on the triplet surface and endothermic by 205.9 kJ/mol on the quintet surface. The second product channel from IM2 is the cleavage of the S−Nb bond resulting in the Nb^+−C−S species. This channel is calculated to be endothermic by 198.3 kJ/mol on the quintet surface and 206.7 kJ/mol on the triplet. This result is in good agreement with early experiments, where the cross section for the formation of NbS^+ is larger than that for $NbCS^+$ at low energy [14].

Obviously, the reaction of Nb^+ with CS_2 proceeds according to the insertion-elimination mechanism. No evidence of other mechanisms has been obtained.

C. Potential surface crossing seam and MECP

The energy profile along the C−S bond activation branch from the reaction of Nb^+ with CS_2 is summarized in Fig.2. Because the ground states of the reactants are quintets and the products are triplets, one must consider the possibility that spin-orbit interaction causes hopping from the quintet surface to the triplet surface. It is well known that transition metal mediated reactions very often occur on more than one PES [17-20]. Spin inversion is a nonadiabatic process, and we need to inspect a crossing seam on the quintet and triplet potential energy surfaces to know the mechanism of the reaction of Nb^+ with CS_2 . The potential energy of the system that consists of four atoms is a function of internal degree of freedom of dimension 6. The crossing seam between the two potential energy surfaces is therefore a "line" of dimension 5, and it is difficult to perform a detailed inspection of the crossing seam as a practical example. Thus, we performed single-point computations of the quintet state as a function of the structural change along the IRC of the triplet state and vice versa, and we obtained the CP along the IRC of the quintet state [26].

Figure 3 shows computed potential energy profiles of the triplet and the quintet states, as a function of the structural change along the quintet IRC respectively. As shown in Fig.3, crossing point is located at S=−5.3 amu$^{1/2}$·bohr, where the two spin states have the same energy and the same structure. Also, the CP was optimized with a separate program linked to the Jaguar QM software. The energy of MECP is −890.432 Hartree. The geometrical parameters are listed in Fig.1. The quintet and triplet potential energy surfaces can begin to touch at this point. After passing MECP, the triplet potential energy surface can provide a low-cost reaction pathway toward the product complex.

D. Reaction mechanism

Figure 4 showes processes of reaction Nb^+ with CS_2. Figure 4 (a) and (b) are the reaction mechanism for Nb^+

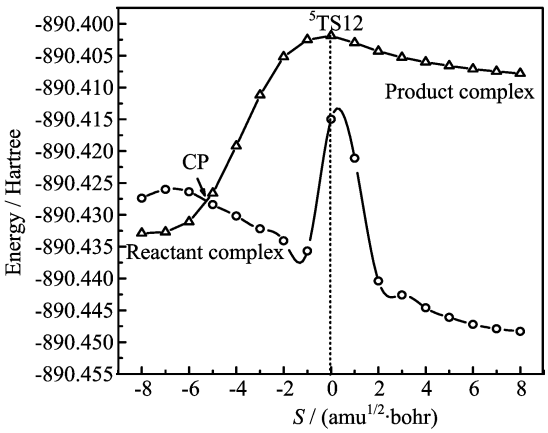

FIG. 3 Potential energies curve-crossing diagram for state correlation between triplet (○) and quintet (△) state.

with CS_2 along the C−S bond activation on triplet PES, on quintet PES respectively. The process is discussed above in detail so it will be ignored.

Because of spin-orbit interaction, the process of forming ground product $^3NbS^+$+^1CS may be: ^5Nb+ CS_2→^{5}IM1→MECP→^{3}IM1→^{3}TS12→^{3}IM2→$^3NbS^+$+ ^{1}CS. We summarize in Fig.5 some features of the quintet and the triplet potential energy surfaces as a vertical sectional view along the reaction pathway for the title reactions. The ground state of the reactant complex is quintet. The potential energy surface of the quintet state gets into contact with the triplet IRC valley at MECP before moving to the transition state, so it is a typical "two-state reactivity" reaction [15]. After passing MECP, the triplet potential energy surface lies completely below the quintet potential energy surface. The spin inversion occurs in this crossing seam, resulting in forming ground state product $^3NbS^+$+^{1}CS.

E. Reaction of CS_2 with Nb^+ *vs.* its reaction with Sc^+, Ti^+, and V^+

The reaction of V^+, Sc^+, and Ti^+ with CS_2 have been reported [10,11], where the C−S bond activation was rationalized according to the insertion-elimination mechanism. From the present study, we found this mechanism also applies to the reaction of Nb^+ with CS_2. From the similarity of the reactions of Sc^+, Ti^+, V^+, and Nb^+ with CS_2, we propose that the reactions of early transition metal ions with CS_2 could proceed via a similar insertion-elimination mechanism. For the reactions of V^+ and Nb^+ with CS_2, the energetically most favorable reaction channel is $^5V^+$+$^1CS_2$→$^3VS^+$+^{1}CS, which is endothermic. However, the reaction $^5Nb^+$+$^1CS_2$→$^3NbS^+$+^{1}CS is exothermic by 2.9 kJ/mol.

Further, all the reactions of Sc^+, Ti^+, V^+, and Nb^+ with CS_2 were found to be "two-state reactivity" reac-

DOI:10.1088/1674-0068/22/03/297-302

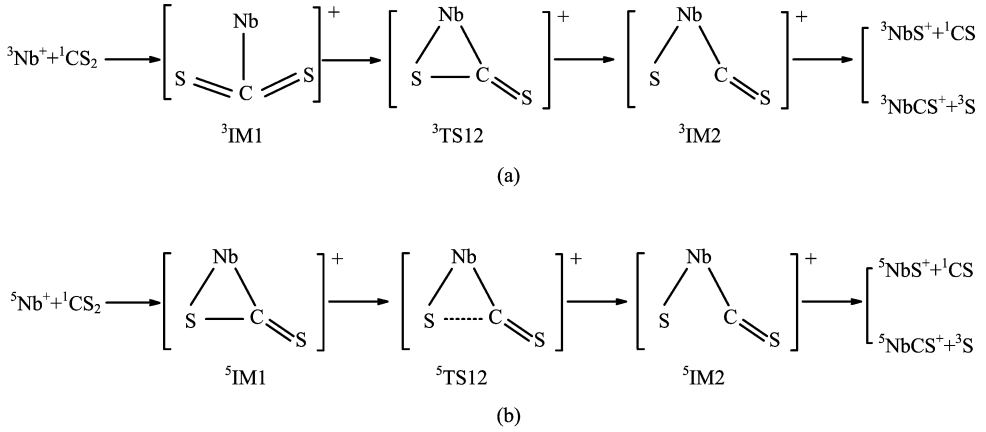

FIG. 4 Proposed reaction mechanism for Nb^+ with CS_2 on triplet (a) and quintet (b) PES.

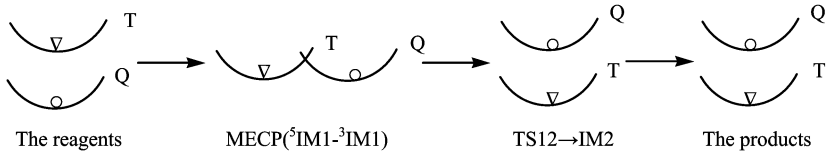

FIG. 5 Vertical sectional views of the quintet (○) and triplet (▽) potential energy surfaces along the reaction pathway.

tions, and the intersystem crossing between two PESs should also occur in the course of early transition metal ions inserting into C−S to lead the system to the energetically most favorable reaction pathway.

IV. CONCLUSION

In this work we present a DFT study of the reaction of Nb^+ with CS_2, which is a representative system selected for the reactions of second-row early transition metal ions with CS_2. The reaction of Nb^+ with CS_2 proceeds according to the insertion-elimination mechanism but not the abstraction mechanism. We found that the reaction of Nb^+ with CS_2 is exothermic by 2.9 kJ/mol. The present calculations support the findings of early experiments. ISC between the two surfaces of $[Nb, C, S]^+$ does occur, and the MECP was found.

[1] E. I. Stiefel, *In ACS Symposium Series*, E. I. Stiefel, and K. Matsumoto, Ed., Washington, DC: American Chemical Society, 2 (1996), and references therein.
[2] K. K. Pandey, Coord. Chem. Rev. **140**, 37 (1995).
[3] S. Takakuwa, *In Organic Sulfur Chemistry, Biochemical Aspects*, S. Oae and T. Okyama, Ed., Boca Raton, FL: CRC Press, (1992).
[4] R. H. Holm, Chem. Rev. **96**, 2237 (1996).
[5] W. Kaim and B. Schwederski, *Bioinorganic Chemistry: Inorganic Elements in the Chemistry of Life*, New York: John Wiley & Sons, (1994).
[6] T. Kondo and T. Mitsudo, Chem. Rev. **100**, 3205 (2000).
[7] M. Almond, B. Cockayne, S. A. Cooke, D. A. Pice, P. C. Smith, and P. J. Wright, J. Mater. Chem. **6**, 1639 (1996).
[8] C. Rue, P. B. Armentrout, I. Kretzschmarz, D. Schröder, and H. Schwarz, J. Phys. Chem. A **106**, 9788 (2002).
[9] Y. C. Wang, L. G. Gao, Z. Y. Geng, X. X. Chen, L. L. Lv, G. L. Dai, and D. M. Wang, Acta Chim. Sin. **63**, 1489 (2005).
[10] L. G. Gao, Y. C. Wang, Z. Y. Geng, X. X. Chen, L. L. Lv, G. L. Dai, and D. M. Wang, Acta Phys. Chim. Sin. **21**, 1102 (2005).
[11] C. Rue, P. B. Armentrout, I. Kretzschmarz, D. Schröder, J. N. Jeremy, and H. Schwarz, J. Chem. Phys. **110**, 7558 (1999).
[12] N. Jiang and D. J. Zhang, Chem. Phys. Lett. **366**, 253 (2002).
[13] C. Rue, P. B. Armentrout, I. Kretzschmarz, D. Schröder, and H. Schwarz, J. Phys. Chem. A **105**, 8456 (2001).
[14] I. Kretzschmarz, D. Schröder, H. Schwarz, C. Rue, and P. B. Armentrout, Int. J. Mass Spectrum **249-250**, 263 (2006).
[15] D. Schröder, S. Shaik, and H. Schwarz, Acc. Chem. Res. **33**, 139 (2000).
[16] K. Yoshizawa, Y. Shiota, and T. Yamabe, J. Chem. Phys. **111**, 538 (1999).
[17] P. B. Armentrout, Science **251**, 175 (1991).
[18] E. R. Davidson, Chem. Rev. **100**, 351 (2000).
[19] M. Torrent, M. Sola, and G. Frenking, Chem. Rev. **100**, 439 (2000).
[20] M. J. Frisch, G. W. Trucks, H. B. Schlegel, G. E. Scuseria, M. A. Robb, J. R. Cheeseman, J. A. Montgomery,

DOI:10.1088/1674-0068/22/03/297-302

Jr., T. Vreven, K. N. Kudin, J. C. Burant, J. M. Millam, S. S. Iyengar, J. Tomasi, V. Barone, B. Mennucci, M. Cossi, G. Scalmani, N. Rega, G. A. Petersson, H. Nakatsuji, M. Hada, M. Ehara, K. Toyota, R. Fukuda, J. Hasegawa, M. Ishida, T. Nakajima, Y. Honda, O. Kitao, H. Nakai, M. Klene, X. Li, J. E. Knox, H. P. Hratchian, J. B. Cross, C. Adamo, J. Jaramillo, R. Gomperts, R. E. Stratmann, O. Yazyev, A. J. Austin, R. Cammi, C. Pomelli, J. W. Ochterski, P. Y. Ayala, K. Morokuma, G. A. Voth, P. Salvador, J. J. Dannenberg, V. G. Zakrzewski, S. Dapprich, A. D. Daniels, M. C. Strain, Ö. Farkas, D. K. Malick, A. D. Rabuck, K. Raghavachari, J. B. Foresman, J. V. Ortiz, Q. Cui, A. G. Baboul, S. Clifford, J. Cioslowski, B. B. Stefanov, G. Liu, A. Liashenko, P. Piskorz, I. Komaromi, R. L. Martin, D. J. Fox, T. Keith, M. A. Al-Laham, C. Y. Peng, A. Nanayakkara, M. Challacombe, P. M. W. Gill, B. Johnson, W. Chen, M. W. Wong, C. Gonzalez, and J. A. Pople, *Gaussian* 03 (*Revision B*.01), Pittsburgh, PA: Gaussian, Inc., (2003).

[21] A. D. Becke, J. Chem. Phys. **98**, 1372 (1993).

[22] C. Lee, W. Ying, and R. G. Parr, Phys. Rev. B **37**, 785 (1998).

[23] E. R. Davidson, Chem. Rev. **100**, 351 (2000).

[24] M. Pavlov, P. E. M. Siegbahn, and M. Sandstrom, J. Phys. Chem. A **102**, 219 (1998).

[25] C. Gonzalez and H. B. Schlegel, J. Chem. Phys. **90**, 2154 (1989).

[26] D. R. Yarkony, J. Am. Chem. Soc. **114**, 5406 (1992).

[27] J.N. Harvey, M. Aschi, H. Schwarz, and W. Koch, Theor. Chem. Accts. **99**, 95 (1998).

[28] L.Gracia, J. Andrés, V. S. Safont, A. Beltrán, and J. R. Sambrano, Organometallics **23**, 730 (2004).

[29] L. G. Gao, X. L. Song, X. X. Chen, and Y. C. Wang, Acta Phys. Chim. Sin. **24**, 2083 (2008).

[30] L. Schröderinger, *Jaguar* 5.5, Portland, (1991-2003).

[31] J. B. Pedley, R. D. Naylor, and S. P. Kirby, *Thermochemical Data of Organic Compounds*, London: Chapman and Hall, (1986).

[32] D. A. Prinslow and P. B. Armentrout, J. Chem. Phys. **94**, 3563 (1991).

[33] R. G. Parr and W. Yang, *Density Functional Theory of Atom and Molecules*, Oxford: Oxford University Press, (1989).

[34] E. S Kryachko and E. V. Ludena, *Electron Density Functional Theory of Many-Electron Systems*, Dordrecht: Kluwer, (1990).

[35] Q. Zhang and M. T. Bowers, J. Phys. Chem. A **108**, 9755 (2004).

[36] P. D. Bolton, E. Clot, A. R. Cowley, and P. Mountford, J. Am. Chem. Soc. **128**, 15005 (2006).

DOI:10.1088/1674-0068/22/03/297-302